

Brownian Motion on a Sphere: Distribution of Solid Angles

M. M. G. Krishna^{1,2}, Joseph Samuel³ and Supurna Sinha⁴

¹Department of Chemical Sciences

Tata Institute of Fundamental Research, Mumbai 400 005, INDIA.

²Department of Biochemistry and Biophysics,

University of Pennsylvania School of Medicine,

Philadelphia, PA 19104, U.S.A.

³Raman Research Institute, Bangalore 560 080, INDIA.

⁴307, Sampige Road #6 Malleswaram, Bangalore 560 003, INDIA.

PACS numbers: 05.40.-a, 03.65.Bz, 05.10.Ln

email: mmg@hxiris.med.upenn.edu, sam@rri.ernet.in

Abstract

We study the diffusion of Brownian particles on the surface of a sphere and compute the distribution of solid angles enclosed by the diffusing particles. This function describes the distribution of geometric phases in two state quantum systems (or polarised light) undergoing random evolution. Our results are also relevant to recent experiments which observe the Brownian motion of molecules on curved surfaces like micelles and biological membranes. Our theoretical analysis agrees well with the results of computer experiments.

Let a diffusing particle start from the north pole of a sphere at time $\tau = 0$. We join the final position of the particle at time β to its initial one (the north pole) by the shorter geodesic. This rule is well defined, unless the final position is *exactly* at the south pole, a zero probability event. The path followed by the diffusing particle (closed by the geodesic rule) encloses a solid angle Ω . The question we address is: At time β , what is the distribution $P^\beta(\Omega)$ of solid angles?

An experimental motivation for this question comes from recent time-resolved fluorescence studies[1, 2, 3, 4] on the Brownian motion of rod-like molecules on curved surfaces such as micelles and lipid vesicles. The experimentally measured fluorescence anisotropy is affected by the curvature of the surface due to geometric phase effects[1, 8, 9]. The problem of diffusion on curved surfaces reappears in Nuclear Magnetic Resonance (NMR) and Electron Spin Resonance (ESR) studies on micelles and lipid vesicles. The curvature of the surface affects the spin relaxation times[5, 6, 7]. In biological systems, the translational diffusion of solutes bound to various curved surfaces influences metabolic rates and transmission rates of chemical signals[1, 7]. Recently, fluorescence anisotropy decay of molecules on curved surfaces has been studied theoretically and using Monte Carlo simulations[1]. This study shows that the geometric phase crucially affects the anisotropy decay if the molecules are tilted relative to the surface normal. We therefore need to theoretically evaluate the distribution of geometric phases or equivalently, the distribution of solid angles in order to understand diffusion processes on curved surfaces.

In this paper we present an answer to the question posed above and compare our theoretical results with Monte Carlo simulations. The theoretical analysis presented here is based on an earlier paper [10] which computes the distribution of solid angles for *closed* Brownian paths. However, closed Brownian paths are a set of measure zero among Brownian paths and a comparison of the results of [10] with real or computer experiments is hampered by poor statistics. We adapt the methods of [10] to allow for *open* Brownian paths and compute the distribution of solid angles for such paths, closing the path by the geodesic rule [8] in order to make the solid angle a well-defined quantity. The qualitative idea behind [10] and the present paper is to use a magnetic field as a “counter”, to measure the solid angle enclosed in a Brownian Motion.

We first illustrate our method by solving a similar problem on the plane. Let a diffusing particle start from the origin $\vec{r} = 0$ of the plane at time $\tau = 0$. Let us suppose that the particle arrives at \vec{r}_f at time β . Join \vec{r}_f to the origin by a straight line. The open Brownian

path $\vec{r}(\tau)$ closed by a straight line encloses an area A . What is the probability distribution $P(A)$ of areas? By “area” we mean the algebraic area, including sign. Area enclosed to the left of the diffusing particle counts as positive and area to the right as negative. This problem has been posed and solved [11] earlier. We illustrate our method by solving this problem before moving to the problem of main interest in this paper.

Let $\{\vec{r}(\tau) = \{x(\tau), y(\tau)\}, 0 \leq \tau \leq \beta, \vec{r}(0) = \vec{0}\}$ be a realization of a Brownian path on the plane which starts at the origin. As is well known, Brownian paths are distributed according to the Wiener Measure [12]: if $\mathcal{F}[\vec{r}(\tau)]$ is any functional on paths, the expectation value of \mathcal{F} is given by

$$\langle \mathcal{F}[\vec{r}(\tau)] \rangle_{\mathcal{W}} := \frac{\int d\vec{r}_f \int \mathcal{D}[\vec{r}(\tau)] \mathcal{F}[\vec{r}(\tau)] \exp[-\int_0^\beta \{\frac{1}{2} \frac{d\vec{r}}{d\tau} \cdot \frac{d\vec{r}}{d\tau} d\tau\}]}{\int d\vec{r}_f \int \mathcal{D}[\vec{r}(\tau)] \exp[-\int_0^\beta \{\frac{1}{2} \frac{d\vec{r}}{d\tau} \cdot \frac{d\vec{r}}{d\tau} d\tau\}]} \quad (1)$$

In Eq. (1) the symbol $\mathcal{D}[\vec{r}(\tau)]$ denotes a functional integral [13] over all paths which start at the origin and end at \vec{r}_f . Finally, the endpoint \vec{r}_f is also integrated over. (We set the diffusion constant equal to half.) β is the time for which the diffusion has occurred [14]. Let $\mathcal{A}[\vec{r}(\tau)]$ be the algebraic area enclosed by the path $\vec{r}(\tau)$. Clearly, the normalized probability distribution of areas $P(A)$ is given by

$$P(A) := \langle \delta(\mathcal{A}[\vec{r}(\tau)] - A) \rangle_{\mathcal{W}}. \quad (2)$$

The expectation value $\bar{\phi}$ of any function $\phi(A)$ of the area is given by $\int P(A)\phi(A)dA$. As is usual in probability theory, we focus on the generating function $\tilde{P}(B)$ of the distribution $P(A)$:

$$\tilde{P}(B) := \overline{e^{iBA}} = \int P(A)e^{iBA}dA, \quad (3)$$

which is simply the Fourier transform of $P(A)$. For reasons that will soon be clear, we use the symbol B for the Fourier transform variable. The distribution $P(A)$ can be recovered from its generating function by an inverse Fourier transform. From Eqs.(2) and (3) above we find

$$\tilde{P}(B) = \langle e^{iBA} \rangle_{\mathcal{W}} \quad (4)$$

Let us introduce a fictitious vector potential $\vec{A}.d\vec{r} = (B/2)(xdy - ydx)$. Clearly $\oint \vec{A}.d\vec{r} = BA$, where the integral is over the closed circuit consisting of the Brownian path closed by the geodesic. \vec{A} has been chosen so that its radial component $\vec{A}.\vec{r}$ vanishes and consequently the contribution of $\int \vec{A}.d\vec{r}$ along the geodesic segment from \vec{r}_f to

$\vec{0}$ vanishes. It follows that $B\mathcal{A}$ can be expressed as

$$B\mathcal{A}[\vec{r}(\tau)] = \int_0^\beta \vec{A}(\vec{r}(\tau)) \cdot \frac{d\vec{r}(\tau)}{d\tau} d\tau, \quad (5)$$

Eqs.(1), (4) and (5) yield

$$\tilde{P}(B) = \frac{\int d\vec{r}_f \int \mathcal{D}[\vec{r}(\tau)] \exp[\int_0^\beta \{-\frac{1}{2} \frac{d\vec{r}}{d\tau} \cdot \frac{d\vec{r}}{d\tau} d\tau\} + i \int_0^\beta \{\vec{A} \cdot \frac{d\vec{r}}{d\tau} d\tau\}]}{\int d\vec{r}_f \int \{\mathcal{D}[\vec{r}(\tau)] \exp[\int_0^\beta \{-\frac{1}{2} \frac{d\vec{r}}{d\tau} \cdot \frac{d\vec{r}}{d\tau} d\tau\}]} \quad (6)$$

By inspection of Eq.(6) we arrive at:

$$\tilde{P}(B) = \frac{Y(B)}{Y(0)}, \quad (7)$$

where $Y(B)$ is given by $Y(B) = \int d\vec{r}_f K^B(\vec{0}, \vec{r}_f)$, where $K^B(\vec{0}, \vec{r}_f)$ is the quantum amplitude for a particle of unit charge and mass to go from the origin $\vec{0}$ to \vec{r}_f in imaginary time β in the presence of a homogenous magnetic field. This amplitude can also be expressed as [13]

$$K^B(\vec{0}, \vec{r}_f) = \sum_{\{n\}} \exp[-\beta E_n] u_n^*(\vec{0}) u_n(\vec{r}_f), \quad (8)$$

where $u_n(\vec{r})$ are a complete set of normalised eigenstates of the Hamiltonian $\hat{H} = (1/2)(-i\vec{\nabla} - \vec{A})^2$ and E_n are the corresponding eigenvalues. (Throughout this paper we set $\hbar = c = 1$.) We thus arrive at the expression: $Y(B) = \int d\vec{r}_f \sum_{\{n\}} \exp - [\beta E_n] u_n^*(\vec{0}) u_n(\vec{r}_f)$.

Now we demonstrate the utility of Eq.(7) by computing the distribution of areas for diffusion on a plane. The function $Y(B)$ for a particle of unit mass and charge in a constant magnetic field, is easily computed[15] from the energies $E_n = (n + \frac{1}{2})B$ and the eigenfunctions $u_n(\vec{r}_f) = \sqrt{B} \exp [(-B/4)r_f^2] L_n[(B/2)r_f^2]$ with L_n , the n^{th} Laguerre polynomial. r_f is the modulus of the vector \vec{r}_f .

$$Y(B) = \frac{2\pi}{\cosh(\frac{\beta B}{2})}.$$

From (7) we find $\tilde{P}(B) = [\cosh(\beta B/2)]^{-1}$. Taking the Fourier transform of $\tilde{P}(B)$ by contour integration we get the result $P(A) = [\beta \cosh(\pi A/\beta)]^{-1}$ as derived in [11]. This provides a check on Eq.(7) and illustrates its use.

Let us now address the problem posed at the beginning of this paper: What is the distribution $P(\Omega)$ of solid angles (Ω) enclosed by a Brownian particle starting at time $\tau = 0$ at the north pole \hat{r}_n of an unit sphere and ending at any other point \hat{r}_f on the sphere, the final point being joined to the initial one by a geodesic. (As stated earlier this

rule breaks down only if the final point is the south pole, which is a zero probability event). Unlike the planar case, $P(\Omega)$ is a periodic[16] function with period 4π . The generating function \tilde{P}_g of the distribution of solid angles is given by

$$\tilde{P}_g = \int_0^{4\pi} d\Omega P(\Omega) e^{ig\Omega} \quad (9)$$

with g a half integer[17]. $P(\Omega)$ is expressed in terms of \tilde{P}_g by a Fourier series (rather than an integral) with g ranging from $-\infty$ to ∞ in half integer steps:

$$P(\Omega) = \frac{1}{4\pi} \sum_{g=-\infty}^{\infty} e^{-ig\Omega} \tilde{P}_g. \quad (10)$$

Relation (7) now takes the form

$$\tilde{P}_g = \frac{Y_g}{Y_0}, \quad (11)$$

where Y_g is given by $Y_g = \int d\hat{r}_f \sum_{\{j,m\}} \exp - [\beta E_{j,m}^g] u_{j,m}^{*g}(\hat{r}_n) u_{j,m}^g(\hat{r}_f)$ with $u_{j,m}^g(\hat{r}_f)$ the normalised eigenfunctions and $E_{j,m}^g$ the energy eigenvalues for a quantum particle of unit charge on a sphere subject to a magnetic field created by a monopole of quantized strength g [18] at the center of the sphere. The quantum numbers of the eigenstates are j, m , where j is the total angular momentum quantum number and m is its z component. We choose the vector potential in the form $A_\phi = g(1 - \cos \theta)$, $A_\theta = 0$, which is non singular everywhere on the sphere except the south pole. Since A_θ vanishes, (as A_r did in the planar case), $\int A$ along the open Brownian path does measure the solid angle as defined by the geodesic rule[8].

The Hamiltonian for this problem is $\hat{H}^g = -\frac{1}{2} \frac{1}{\sin \theta} \frac{\partial}{\partial \theta} \sin \theta \frac{\partial}{\partial \theta} + (-i \frac{\partial}{\partial \phi} - A_\phi^g)^2$ in standard spherical co-ordinates. The wave equation can be separated by writing $\psi(\theta, \phi) = \exp(ip_\phi \phi) R(\theta)$. From continuity of ψ , it follows that $R(0) = 0$ if $p_\phi \neq 0$. Therefore, only those eigenstates for which $p_\phi = 0$, contribute to Y^g . These normalised eigenstates are labelled by j , which ranges from $|g|$ to ∞ in integer steps.

$$R_j^g(z) = \sqrt{\frac{2j+1}{2}} \frac{1}{2^g} (1+z)^g P^{0,2g}_{j-g}(z), \quad (12)$$

where $z = \cos \theta$ and $P_n^{a,b}$ are the Jacobi Polynomials [19]. The energy levels of this system are [20, 19]: $E_j^g = \frac{j(j+1)-g^2}{2}$. Using the integer $n = j - |g|$ to label the states (in place of j) we find

$$\tilde{P}^g = \sum_{n=0}^{\infty} (-1)^n \exp(-[n(n+1) + g(2n+1)]\beta/2) \frac{(2n+2g+1)g}{(g+n)(g+n+1)}, \quad (13)$$

for $g > 0$ and $\tilde{P}^0 = 1$. From (10) we arrive at [21]

$$P(\Omega) = (1/4\pi)(1 + 2 \sum_{g=1/2}^{\infty} \cos(\Omega g) \tilde{P}_g), \quad (14)$$

where g increases in half integer steps. The function (14) is plotted numerically for various values of β in Fig. 1. The qualitative nature of these plots is easily understood. For small values of β the particle tends to make small excursions and its path encloses solid angles close to 0 or 4π and consequently the plots are peaked around these two values. As the available time β increases, other values of Ω are also probable and the peaks tend to spread and the curves to flatten out. Finally in the limit of $\beta \rightarrow \infty$ the particle has enough time to enclose all possible solid angles with equal probability. These plots give the answer to the question that was raised in the beginning of the paper.

The analytical solution given above was checked against the results of computer experiments. The diffusion process was simulated on a Silicon Graphics workstation by Monte Carlo methods. The simulation methodology was adapted from [1] (where more details are given) and is briefly as follows. We start the simulation with 10^5 molecules located at the north pole of a sphere with all molecular dipoles aligned parallel to the spherical surface (perpendicular to the position vectors). Let \hat{V}_0 represent the dipoles at zero time, oriented along the laboratory x-axis which is perpendicular to the position vector \hat{R}_0 along the laboratory z-axis. These molecules are then subjected to random “kicks” and allowed to diffuse over the sphere independent of each other. The diffusion of the dipoles on the spherical surface is effected by rotation of the position vector \hat{R} and the dipole vector \hat{V} by the same three dimensional rotation matrix about a randomly chosen vector \hat{n} normal to the radial position vector \hat{R} . In the simulation, the diffusion constant D is chosen to be 10^{-3} per time step and the angle of rotation per time step (one iteration) is obtained from the corresponding probability equation for planar diffusion, which is valid for very small diffusion lengths. The orientation of the molecule \hat{V} during diffusion is used as an index of the solid angle swept out by the Brownian path. We numerically evaluate this for each molecule applying the geodesic rule. Let \hat{V}_β and \hat{R}_β represent the dipole and the radial vectors at time β . To determine the orientation of \hat{V}_β , \hat{V}_β is transformed to \hat{V}'_β using a three dimensional rotation matrix with an angle of rotation (less than π) determined by $\cos^{-1}(\hat{R}_\beta \cdot \hat{R}_0)$. The angle between \hat{V}'_β and \hat{V}_0 is the solid angle enclosed by the Brownian path of the diffusing molecule at time β . Similarly, the solid angles are calculated for all the 10^5 dipoles at different times. These are sorted into 360 different bins, each

corresponding to one degree increment between 0 and 2π and are plotted in Figure 2.

Since the orientation of the molecule is only determined modulo 2π in the simulation, Ω is only measured modulo 2π and not modulo 4π . So in effect the function computed by the simulation is $Q(\Omega) = P(\Omega) + P(\Omega + 2\pi)$. From (14) it is clear that the half integer values of g cancel out and the integer values are doubled. Our theoretical expression for $Q(\Omega)$ is therefore

$$Q(\Omega) = (1/2\pi)(1 + 2 \sum_{g=1}^{\infty} \cos(\Omega g) \tilde{P}_g), \quad (15)$$

where g now increases in *integer* steps. The results of the numerical simulation and the function $Q(\Omega)$ (with suitable cutoffs on g and n) given above are plotted in Figure 2 for different values of β . The agreement between the simulations and the theory is excellent and the fractional deviation is of order $1/\sqrt{N}$ where N is the number of molecules in a bin.

In computing the distribution of solid angles, we have chosen all the molecules to be initially at the north pole ($\hat{r}_i = \hat{r}_n$) and integrated over the final point \hat{r}_f with a uniform weight, to match with the procedure followed in our simulation. In an experimental situation, where the diffusing particles are excited and observed with external probes, it may be necessary to consider a weighted average over the initial and final positions of the diffusing particles [1]. Our analysis is easily adapted to take this into account. One just writes

$$Y^g = \int d\hat{r}_f w_f(\hat{r}_f) d\hat{r}_i w_i(\hat{r}_i) K^g(\hat{r}_i, \hat{r}_f). \quad (16)$$

This leads to $Y^g = \sum_n w^{g*}_i w^g_f \exp[-\beta E_n^g/2]$, where $w^g_n = \int d\hat{r} w(\hat{r}) u_n^g(\hat{r})$ and the sum is over all eigenstates. In this paper we have set $w_i(\hat{r}_i) = \delta^2(\hat{r}_i - \hat{r}_n)$ and $w_f(\hat{r}_f) = 1$.

In the problem of diffusion of fluorescent molecules, the tangential component of the orientation of the molecule determines the solid angle enclosed by the diffusing particle only modulo 2π . This is because, in parallel transport of a vector, the vector rotates by an angle *equal* to the solid angle enclosed by the curve. As Pancharatnam showed [8], a quantum two state system transported on the Poincaré sphere picks up a geometric phase equal to *half* the enclosed solid angle. This measures the solid angle modulo 4π . The distribution $P(\Omega)$ computed in the body of the text describes the distribution of geometric phases. However, since our simulations were adapted from [1], the distribution measured in the simulation is $Q(\Omega)$ and not $P(\Omega)$.

In [10], the generating function for the distribution of solid angles for *closed* Brownian

paths involved *only* the energy eigenvalues of the Hamiltonian. In contrast, in the present case of *open* Brownian paths (closed by the geodesic rule), one needs to use *both* the eigenvalues as well as the *eigenfunctions* of the Hamiltonian. This is the main difference between [10] and the present theoretical analysis.

We have computed the distribution of solid angles for Brownian motion on the sphere. This calculation has also been checked against computer experiments. In simple geometries like the surface of a sphere, an analytical treatment is possible. In more complicated situations, one is forced to rely on computer simulations. Monte Carlo simulations can be used in two distinct roles. In the present problem, where an analytical treatment is possible, simulations can be viewed as a computer experiment against which the theory can be tested. Such experiments are much easier to control than real experiments. In cases where an analytical treatment is not possible, the simulations serve as a substitute for the theory, to be checked against real experiments. The agreement between theory and computer experiments for Brownian motion on the sphere also serves as a check on the computer simulations so that these simulations can be confidently used in geometries which cannot be treated analytically.

Acknowledgements: It is a pleasure to thank R. Nityananda for discussions on this subject and S. Ramasubramanian for drawing our attention to Ref. [11] and Y. Hatwalne for a critical reading of the manuscript. JS and SS thank N. Kumar for raising the question of the distribution of solid angles on a sphere. MMGK thanks N. Periasamy and S.W. Englander for their encouragement.

References

- [1] M. M. G. Krishna, R. Nityananda, R. Das and N. Periasamy, “Translational Diffusion of Fluorescent Probes on a Sphere: Monte Carlo Simulations, Theory and Fluorescence Anisotropy Experiments”, Submitted for publication.
- [2] N. C. Maiti, M. M. G. Krishna, P. J. Britto and N. Periasamy, *J. Phys. Chem. B*, **101** (1997) 11051.
- [3] E. L. Quitevis, A. H. Marcus, and M. D. Fayer, *J. Phys. Chem.*, **97** (1993) 5762.
- [4] N. C. Maiti, S. Mazumdar and N. Periasamy, *J. Phys. Chem.*, **99** (1995) 10708.
- [5] H. Walderhaug, O. Soderman and P. Stilbs, *J. Phys. Chem.*, **88** (1984) 1655.
- [6] H. Nery, O. Soderman, H. Walderhaug and B. Lindman, *J. Phys. Chem.*, **90** (1986) 5802.
- [7] P. W. Kuchel, A. J. Lennon and C. Durrant, *J. Magn. Reson.*, **112** (1996) 1.

- [8] See “Geometric Phases in Physics ” Eds. Alfred Shapere and Frank Wilczek, World Scientific, Singapore (1989).
- [9] J. W. Zwanziger, M. Koenig and A. Pines, *Annu. Rev. Phys. Chem.*, **41** (1990) 601.
- [10] S. Sinha and J. Samuel, *Phys. Rev.* **B 50** (1994) 13871.
- [11] “Stochastic Differential equations and Diffusion Processes” by N. Ikeda and S. Watanabe, North Holland/Kodansha (1981), p387.
- [12] L.S. Schulman, “Techniques and Applications of Path Integration”, John Wiley and Sons, N.Y. (1981).
- [13] R.P. Feynman and A. R. Hibbs, “Quantum Mechanics and Path Integrals”, McGraw-Hill, N. Y. (1965).
- [14] In real applications, β is equal to $2Dt$ in the case of a plane and is equal to $2Dt/R^2$ in the case of a sphere, where D is the diffusion coefficient on the surface, R is the radius and t is the time for which the particle has diffused. In the text we have chosen units so that $R = 1, D = 1/2$ then β is equal to the time.
- [15] L. D. Landau and E. M. Lifshitz, “Quantum Mechanics”, Pergamon Press, Oxford (1977) p 457.
- [16] A path that encloses a solid angle Ω to its left also encloses a solid angle of $4\pi - \Omega$ to its right. Using the symmetry $P(\Omega) = P(-\Omega)$ we conclude that $P(\Omega)$ is periodic with period 4π .
- [17] Note that the definition of g here is *not* the same as in ref. [10], which contains an error: in the equation before (11) g should be replaced by $g/2$. This error propagates to equations (11,12) and Figure 1 but not to the subsequent discussion.
- [18] P. A. M. Dirac, *Proc. Roy. Soc. London* **A133** (1931) 60; M. N. Saha, *Ind. J. Phys.* **10** (1936) 141.
- [19] “Angular Momentum in Quantum Mechanics” by A.R. Edmonds, Princeton University Press, Princeton (1960), pp 58-65.
- [20] S. Coleman, “The Magnetic Monopole Fifty Years Later”, in A. Zichichi, ed., *The Unity of Fundamental Interactions* (New York:Plenum Press, 1983).
- [21] The summation over g *can* be performed analytically, but the resulting expression is not suitable for plotting $P(\Omega)$ or $Q(\Omega)$, since it involves delicate cancellations between separately divergent terms.

Figure Captions

Fig. 1: The solid angle distributions $P(\Omega)$ computed from Eq. 14 at five different values of β : 0.5, 1, 2, 5 and 10. The flatter curves correspond to higher β .

Fig. 2: Comparison between solid angle distributions $Q(\Omega)$ from Monte Carlo simulations (red line) and the theory (Eq. 15) (blue line). The plot shows the distributions at five different values of β : 0.5, 1, 2, 5 and 10.

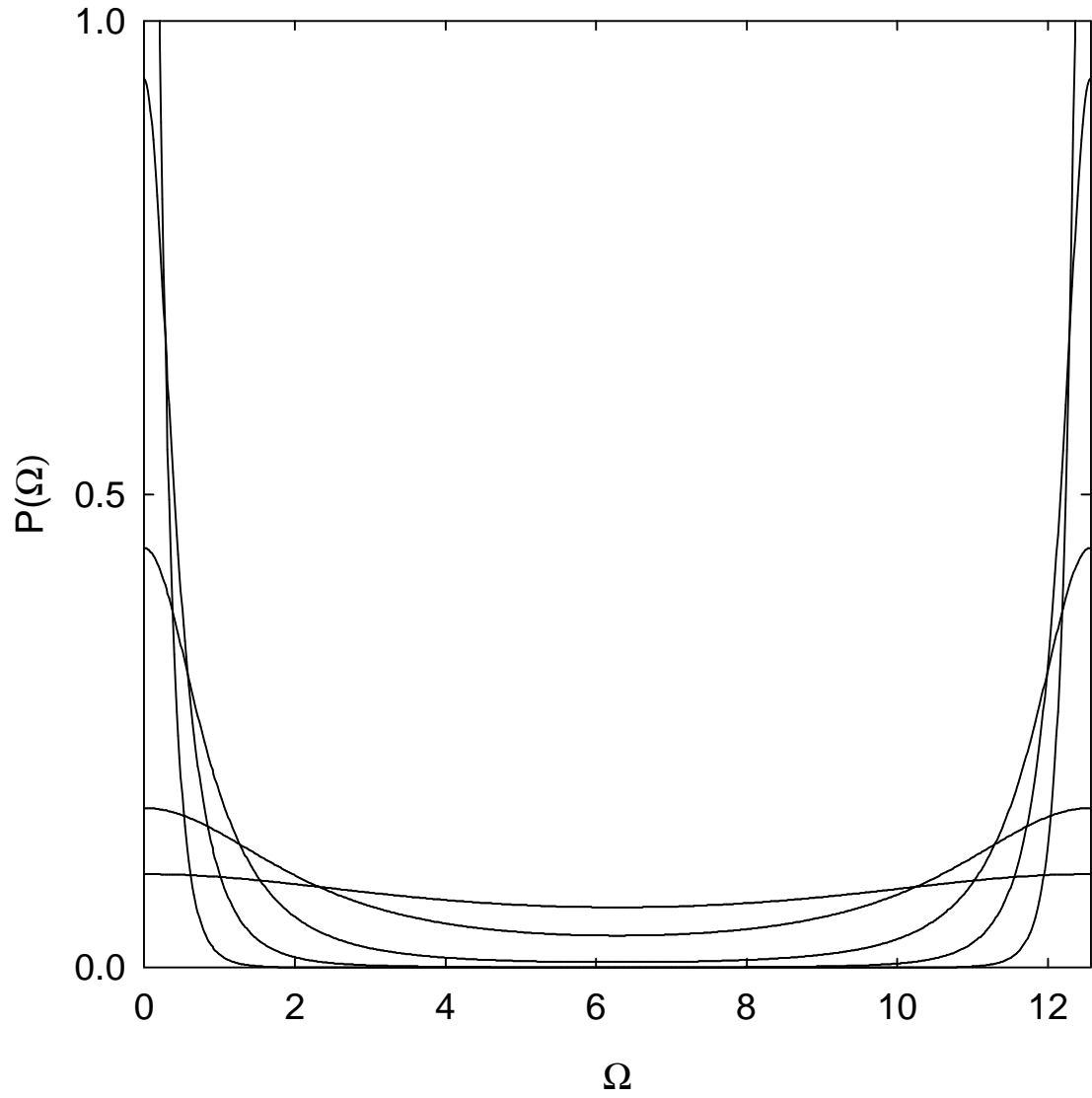


Fig.1

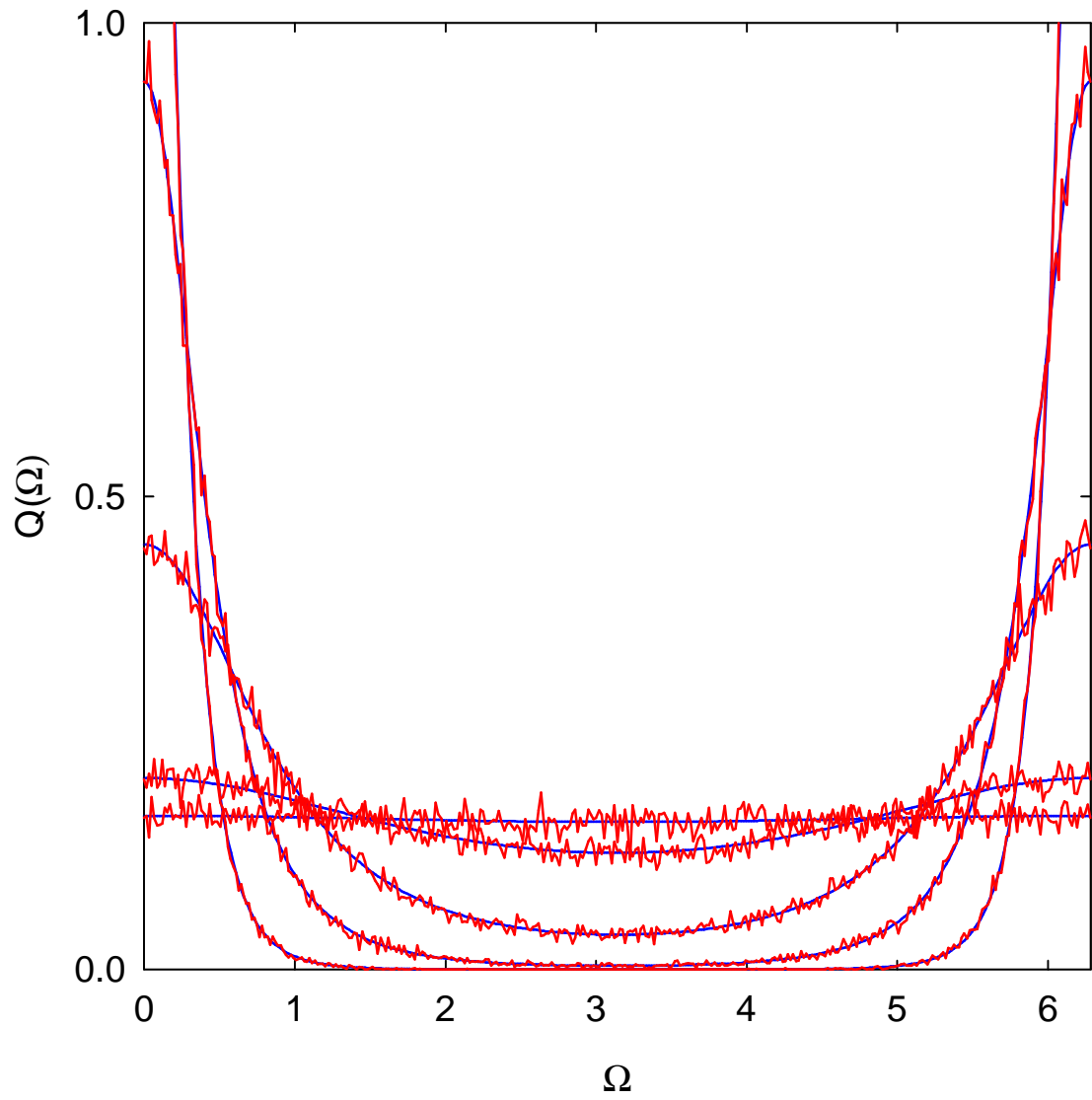


Fig.2